



Journal of Zhejiang University-SCIENCE A (Applied Physics & Engineering)
ISSN 1673-565X (Print); ISSN 1862-1775 (Online)
www.jzus.zju.edu.cn; www.springerlink.com
E-mail: jzus@zju.edu.cn



Effect of valve core shapes on cavitation flow through a sleeve regulating valve^{*}

Zhi-jiang JIN¹, Chang QIU¹, Cheng-hang JIANG², Jia-yi WU¹, Jin-yuan QIAN^{†‡1,3}

¹Institute of Process Equipment, College of Energy Engineering, Zhejiang University, Hangzhou 310027, China

²Hangzhou Special Equipment Inspection & Research Institute, Hangzhou 310051, China

³State Key Laboratory of Fluid Power and Mechatronic Systems, Zhejiang University, Hangzhou 310027, China

[†]E-mail: qianjy@zju.edu.cn

Received Oct. 15, 2019; Revision accepted Dec. 2, 2019; Crosschecked Dec. 17, 2019

Abstract: Cavitation occurring in a sleeve regulating valve not only increases the energy waste of the whole piping system but also causes severe and costly damage to the valve body and the piping system. In this paper, in order to reduce the cavitation inside the sleeve regulating valve, the effects of different valve core shapes, including flat bottom, ellipsoid, circular truncated cone, and cylinder, on cavitation are investigated by using a cavitation model. The pressure, velocity, and vapor volume fraction distribution in the regulating valve are obtained and compared for different valve core shapes and valve core displacements. The total vapor volumes are also predicted and compared. The results show that vapor primarily appears in the gap between the sleeve and the valve core surface. The cavitation intensities for the ellipsoid and cylinder valve cores are greater than those for the other two valve cores. With the increase of the valve core displacement, the total vapor volumes for all four valve core shapes first increase and then decrease. This work is of significance for the optimization and design of sleeve regulating valves.

Key words: Sleeve regulating valve; Cavitation intensity; Valve core shape; Total vapor volume
<https://doi.org/10.1631/jzus.A1900528>

CLC number: TH161.12

1 Introduction

A regulating valve plays an important role in pipeline systems and is widely used in a variety of industries such as power engineering, chemical engineering, and petrifaction. A regulating valve consists of two main parts: the valve body, which

conveys and directs the flow, and the actuator, which provides the necessary force for the movement of the valve components. The flow rate passing through the regulating valve is changed by adjusting the distance between a stationary valve seat and a movable valve core. For a regulating valve, which conveys liquids, cavitation is a serious and destructive problem during its operation because pressure may drop owing to the variation of velocity. If the local pressure is lower than the corresponding saturated vapor pressure at the same temperature, bubbles can form and then grow until bursting. Longtime cavitation flow can not only induce a waste of energy, but also cause the failure of the piping system. Moreover, the lifetime of valves is reduced and noise can also be induced within the cavitation flow. Thus, the investigation of flow and cavitation characteristics inside the regulating valves is necessary.

[‡] Corresponding author

^{*} Project supported by the National Natural Science Foundation of China (No. 51805470), the Zhejiang Provincial Natural Science Foundation of China (No. LY20E050016), the Zhejiang Provincial Key Research & Development Project (No. 2019C01025), the Youth Funds of the State Key Laboratory of Fluid Power and Mechatronic Systems (Zhejiang University) (No. SJKoFP-QN-1801), and the Zhejiang Provincial Quality and Technical Supervision Research Project (No. 20180117), China

ORCID: Zhi-jiang JIN, <https://orcid.org/0000-0002-8063-709X>; Jin-yuan QIAN, <https://orcid.org/0000-0002-5438-0833>

© Zhejiang University and Springer-Verlag GmbH Germany, part of Springer Nature 2020

In the recent years, many researchers have achieved some meaningful results about the internal flow characteristics, pressure control, and structure optimization in regulating valves. Qian et al. (2014) carried out computational fluid dynamics (CFD) analysis on the dynamic flow characteristic of the pilot-control globe valve. Huovinen et al. (2015) studied the turbulent flow inside a choke valve by using CFD and experiments. Edvardsen et al. (2015) paid attention to the pressure drop in a downhole shut-in valve. Corbera et al. (2016) presented a novel multi-objective approach for the design optimization of a butterfly valve using genetic algorithms. Lisowski and Filo (2016) analyzed the flow characteristics of a proportional control valve to improve them by means of geometrical modifications of the valve spool. Qian et al. (2019e) simulated the flow of nanofluids through a micro Tesla valve. Fu et al. (2013) and Wang et al. (2014) introduced a novel valve core structure of a throttle valve and its mathematical model, which was validated by CFD simulations and experiments. Xu et al. (2014) carried out the structural optimization of downhole float valve via CFD. Liu et al. (2019) studied the metrological performance of a swirlmeter affected by flow regulation with a sleeve valve.

For cavitation flow inside the regulating valves, some meaningful studies have also been carried out by experimental and numerical methods. Qian et al. (2019b) carried out a comprehensive review of cavitation in valves including mechanical heart valves and control valves. Wang et al. (2019) analyzed the gas-water two-phase flow in a self-priming centrifugal pump. Gao et al. (2006) studied the cavitation flow through the orifice in a poppet valve and a ball valve numerically and experimentally. Moreover, aimed at the orifice structure, Qian et al. (2019a) researched the fluid flow through multi-stage perforated plates. Liu and Ji (2009) investigated the flow and cavitation characteristics in a rotary valve by CFD. Jia and Yin (2010) investigated the cavitation phenomenon near the port of a cylinder valve experimentally and numerically. Li et al. (2013) analyzed the cavitation phenomenon of an electrohydraulic servo-valve by a numerical method and experimental observations. Ulanicki et al. (2015) introduced a novel method to estimate whether cavitation occurs in the pressure reducing valve. Kudźma and Stosiak (2015)

simulated the cavitation flow through a hydraulic lift valve using the acoustic and visual method. Ou et al. (2015) analyzed the effects of valve core openings and inlet and outlet pressures on cavitation characteristics for a pressure relief valve. Qu et al. (2015) conducted the experiments on flow resistance coefficient of a pressure-regulating valve and predicted the transient cavitation flow for different inlet conditions. Deng et al. (2015) simulated the flow structure and cavitation pattern inside a spool valve for two different flow states. Lu et al. (2020) conducted the numerical simulation and experiments on large vapor cavity produced by a vortex flow in a U-shape notch spool valve. Jin et al. (2018) investigated the effects of different structure parameters on hydrodynamic cavitation characteristics in a globe valve by a numerical method. Pressure loss is a critical factor which influences cavitation. Tao et al. (2020) studied the regulating performance and flow loss in a V-port ball valve. Qian et al. (2019c, 2019d) analyzed the energy loss and pressure loss inside multi-stage Tesla valves. Some researchers concentrated more on the noise induced by cavitation flow. Hassis (1999) analyzed the effects of cavitation on local pressure fluctuation, noise level, and resonance frequency in a butterfly valve and a Monovar valve by experiments. Herbertson et al. (2006) adopted the wavelet functions to denoise the noise signal induced by cavitation and distinct types of cavitation in a mechanical heart valve. Okita et al. (2015) found that the fluctuation of cavitation volume inside a relief valve is corresponding to the downstream pressure fluctuation by a high-speed camera and a numerical method.

Furthermore, some research on the suppression of cavitation has been carried out and some methods have been proposed for suppressing cavitation inside the valve. Nie et al. (2006) analyzed the influences of the passage area ratio of two throttles and the inlet and outlet pressures on pressure distributions and the critical cavitation index in a throttle poppet valve. Baran et al. (2010) introduced a methodology to monitor the cavitation behavior of a valve, which was identified by pressure drop, vibration, and noise level. Zhang et al. (2017) designed a new optimized throttle valve chamber structure and investigated the anti-cavitation of the valve through CFD. Shi et al. (2017) analyzed the effects of the inlet and outlet pressures on the anti-cavitation performance of a water

hydraulic throttle valve experimentally. In addition, multi-stage sleeves were proposed to control cavitation in valves and the effects of them on cavitation performance were investigated by Chern et al. (2013) and Yaghoubi et al. (2018). For the throttling sleeve inside valves, a parametric analysis was conducted by Hou et al. (2018).

In this study, a multiphase cavitation flow model is proposed to simulate the flow and cavitation in a sleeve regulating valve. Four valve core shapes, including flat bottom, ellipsoid, circular truncated cone, and cylinder, are explored to investigate the effects of the valve core shapes on cavitation intensity and the region of cavitation inside the regulating valve. The research work is of interest for optimizing the design of the sleeve regulating valve.

2 Numerical model

2.1 Mathematical model

Flow through the sleeve regulating valve is turbulence because the Reynolds number is higher than 10^5 , and the water and water vapor are considered as working fluids. The standard $k-\varepsilon$ turbulence model is adopted in solving the turbulence flow.

In the cavitation simulations, phase change occurs between the liquid and vapor phases. The simulations are conducted in a steady state. The cavitation model employed here is that proposed by Schnerr and Sauer (2001). The vapor transfer equation is

$$\frac{\partial}{\partial t}(\alpha\rho_v) + \nabla \cdot (\alpha\rho_v \mathbf{v}_v) = R_e - R_c, \quad (1)$$

where t denotes the time, α represents the vapor volume fraction, the subscript v denotes the vapor phase, ρ_v represents the vapor density, \mathbf{v}_v is the vapor velocity vector, and R_e and R_c represent the mass rates of growth and collapse of the vapor bubble given by

$$R_e = \frac{3\alpha\rho_v(1-\alpha)\rho_l}{\rho_m R_b} \sqrt{\frac{2(p_v - p)}{3\rho_l}}, \quad p_v \geq p, \quad (2)$$

$$R_c = \frac{3\alpha\rho_v(1-\alpha)\rho_l}{\rho_m R_b} \sqrt{\frac{2(p - p_v)}{3\rho_l}}, \quad p_v \leq p, \quad (3)$$

where p denotes the local pressure, p_v denotes the saturation vapor pressure of water, ρ_l and ρ_m represent the liquid and mixture densities, respectively, and R_b denotes the bubble radius given by

$$R_b = \left(\frac{\alpha}{1-\alpha} \frac{3}{4\pi n} \right)^{\frac{1}{3}}, \quad (4)$$

where n is related to the bubble number density and is set as 1×10^{13} .

2.2 Geometrical model

Fig. 1a shows the schematic structure of the studied sleeve regulating valve. It consists of a valve body, valve cover, valve core, and the sleeve with orifices. The valve core can move upward and downward vertically, driven by the valve rod and a driving device. The inlet and outlet diameters of the valve are 130 mm and the orifice diameter in the sleeve is 4 mm. In this study, the valve core displacement is varied from 10 mm to 60 mm. With the increase of the valve core displacement, the sleeve regulating valve is opened. Fig. 1b shows the studied valve core structure with different shapes including flat bottom, ellipsoid, circular truncated cone, and cylinder. The valve core in Fig. 1a is the flat bottom one. The valves with different valve core shapes produce different flux characteristics and pressure distributions.

In the numerical simulation, some simplifications are carried out to enable numerical analysis. First, the sleeve regulating valve is assumed as an ideal valve, which means its cutting edge is at a right angle exactly with sharp edges, and the valve core matches the valve seat precisely. Second, a 3D axisymmetric geometric model is adopted considering the symmetry structure to save computing time. At last, the effect of the gravity and heat transfer is not considered.

2.3 Mesh and boundary condition

The 3D flow channel model with a maximum valve core displacement of 60 mm is created in the modeling software SOLIDWORKS. The software, ANSYS Workbench 17.2, is used to generate the mesh of the flow channel. Fig. 2 depicts the generated meshes of the flow channel inside the sleeve regulating

valve. To reduce the influence of the boundary, part of the flow area in the pipeline is also considered. The upstream and downstream pipes are extended to five diameters, 600 mm. Due to the complexity of the flow channel, the mesh of flow channel inside the valve is generated by a non-structure mesh method. The boundary layer meshes are also considered and the thickness of first boundary layer is set as 0.2 mm.

The grid independency is checked taking the valve core displacement of 60 mm with inlet pressure 8.45 MPa as checking condition. Fig. 3 shows the outlet mass flow rate and the vapor volume fraction at the inlet of the sleeve with different grid numbers from 1.5×10^6 to 2.7×10^6 . It indicates that the relative errors are lower than 1% when the grid number is higher than 2.1×10^6 . A grid number of 2.4×10^6 is chosen.

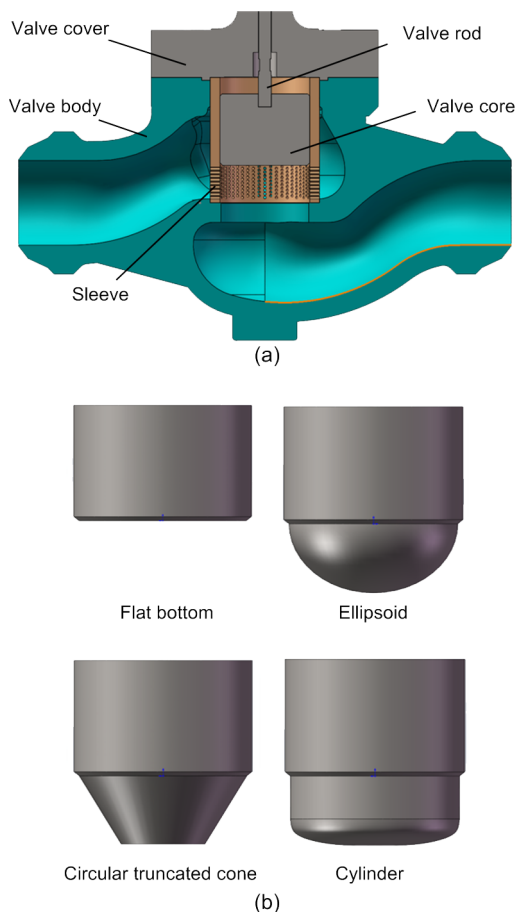


Fig. 1 Schematic structure of the studied sleeve regulating valve

(a) Overall view of the schematic structure; (b) Studied valve cores with different shapes

For the boundary conditions, the pressure inlet and outlet are adopted, and the wall is set as no-slip wall, where the wall function method is adopted. Here, the inlet and outlet pressures are set as 8.45 MPa and 2.00 MPa, respectively. The inlet and outlet conditions both remain constant in the simulations. The inlet vapor volume fraction is set as zero initially. The main work fluid inside the sleeve regulating valve is liquid water at 200 °C. Liquid water and the water vapor are set as the liquid and vapor phases, respectively. Correspondingly, the densities of the liquid and vapor phases, ρ_l and ρ_v , are set as 862.8 kg/m^3 and 7.865 kg/m^3 , and the dynamic viscosities of the liquid and vapor phases, μ_l and μ_v , are set as $1.357 \times 10^{-4} \text{ Pa}\cdot\text{s}$ and $1.565 \times 10^{-5} \text{ Pa}\cdot\text{s}$, respectively. The vaporization pressure of the liquid phase is set as 1.50 MPa, which represents the saturation vapor pressure of water at 200 °C. The numerical model is solved in Fluent 17.2.

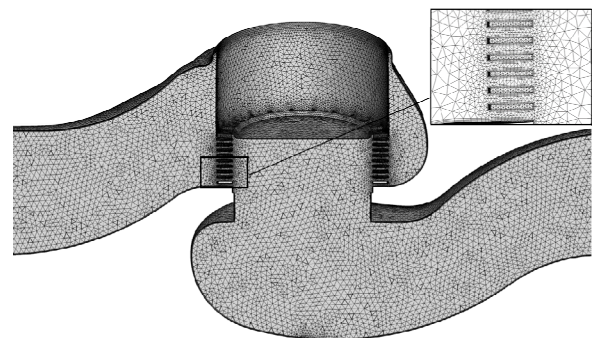


Fig. 2 Meshes of the sleeve regulating valve with maximum valve core displacement of 60 mm

3 Results and discussion

When the fluid flows through the sleeve regulating valve, there are sudden changes in its flow direction and flow velocity, so the pressure and flow fields around the valve core and sleeve become complex and cavitation may occur. For the sleeve regulating valve, the valve core shapes may also influence the cavitation distribution and density, and the effects of valve core shapes on the cavitation are different for different valve core displacements. To analyze the effect of the valve core shapes, the four valve core shapes, i.e. flat bottom, ellipsoid, circular truncated cone, and cylinder, are introduced. The

sleeve regulating valves with these four different valve core shapes for different valve core displacements are analyzed and compared.

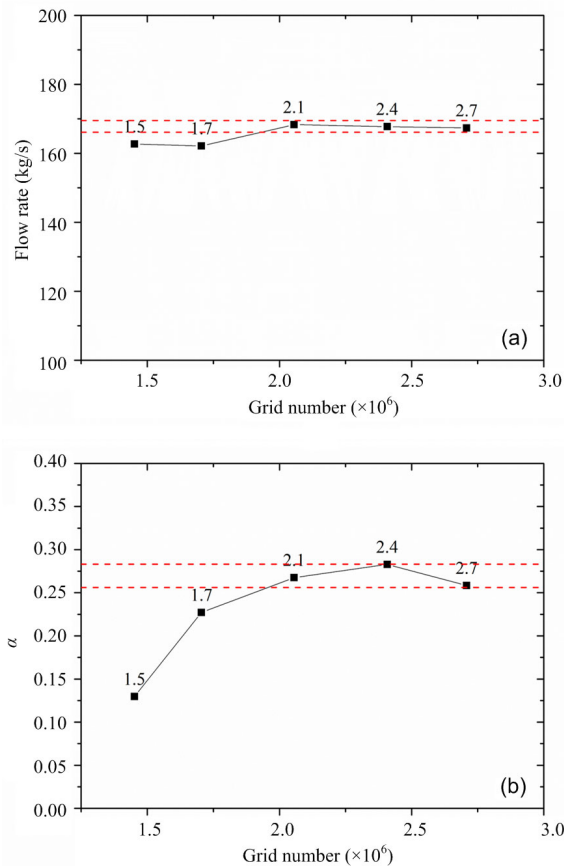


Fig. 3 Grid independency check for different grid numbers

(a) Flow rates for different grid numbers; (b) Vapor volume fractions for different grid numbers

3.1 Velocity and flux analysis on cavitation flow

Fig. 4 shows the velocity contours of the symmetric cross section of valve for different valve core shapes when the valve core displacement is 60 mm, while Fig. 5 depicts the velocity contours with the valve core displacement of 30 mm.

Some similarities can be found in velocity distributions for different valve core shapes in Fig. 4. For all four valve cores, when the fluid flows through the throttling region of the sleeve, there is always a sudden rise of velocity of up to 100 m/s in the orifices. Meanwhile, a vortex can be seen in the left side of the valve chamber and there is always a region of high

velocity in the center of the valve chamber. The velocity difference between the center and left side of the valve chamber induces a vortex in the left side of the valve chamber. However, for the different valve cores, some differences can be found in the velocity distributions. For the flat bottom, ellipsoid, and circular truncated cone valve cores, the inlet velocities are all kept above 20 m/s and the outlet velocities all remain above 20 m/s. But for the cylinder valve core, the inlet and outlet velocities are both kept below 20 m/s. The cylinder valve core induces a significant enhancement of the valve's throttling effect. The energy cost for the cylinder valve core when the fluid flows through the valve is higher than for the other three valve cores. In addition, due to the change in shape of the valve core, a vortex is observed at the bottom of the valve core for the circular truncated cone and cylinder valve cores.

When the valve core displacement is decreased from 60 mm to 30 mm, the effects of the shape of the valve core on the velocity distribution are changed. Not only the velocities at the inlet and outlet of the valve, but also the velocity at the center of the valve chamber is decreased. For the flat bottom and ellipsoid valve cores, the velocities at the inlet and outlet remain above 10 m/s, but for the circular truncated cone and cylinder valve cores, the velocities at the inlet and outlet pass below 10 m/s. It can be seen that the throttling effects of the valve with the flat bottom and ellipsoid valve cores are similar when the valve core displacement is 30 mm. The throttling effects of the valves with circular truncated cone and cylinder valve cores are also similar. In addition, for the circular truncated cone valve core, there are two vortices at the bottom of the valve core, whereas there is only one at the bottom of the cylinder valve core. For the cylinder valve core, the maximum flow velocity appears in the gap between the valve core and the valve chamber wall rather than at the orifice in the sleeve.

Fig. 6 (p.7) depicts the velocity variation along the horizontal direction for different valve core shapes when the valve core displacements are 60 mm and 30 mm. Some further comparisons can be carried out in the velocity distribution along the horizontal direction. For the cylinder valve core, the velocities at the inlet and outlet are significantly lower than for the others, and the velocity in the throttling region is

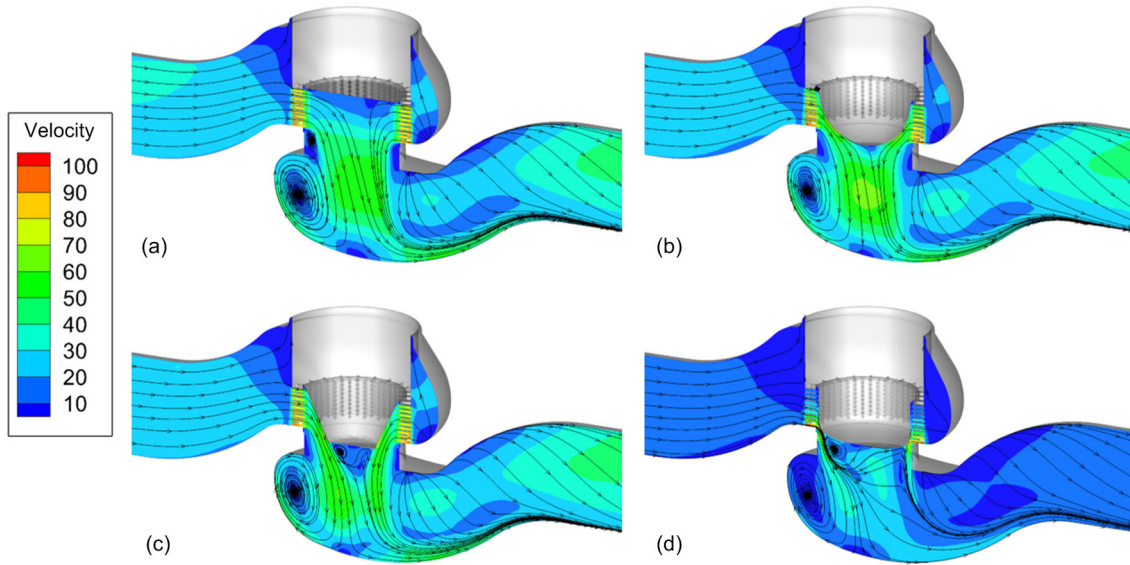


Fig. 4 Velocity (unit: m/s) contours inside the sleeve regulating valve with valve core displacement of 60 mm for different valve core shapes: (a) flat bottom; (b) ellipsoid; (c) circular truncated cone; (d) cylinder

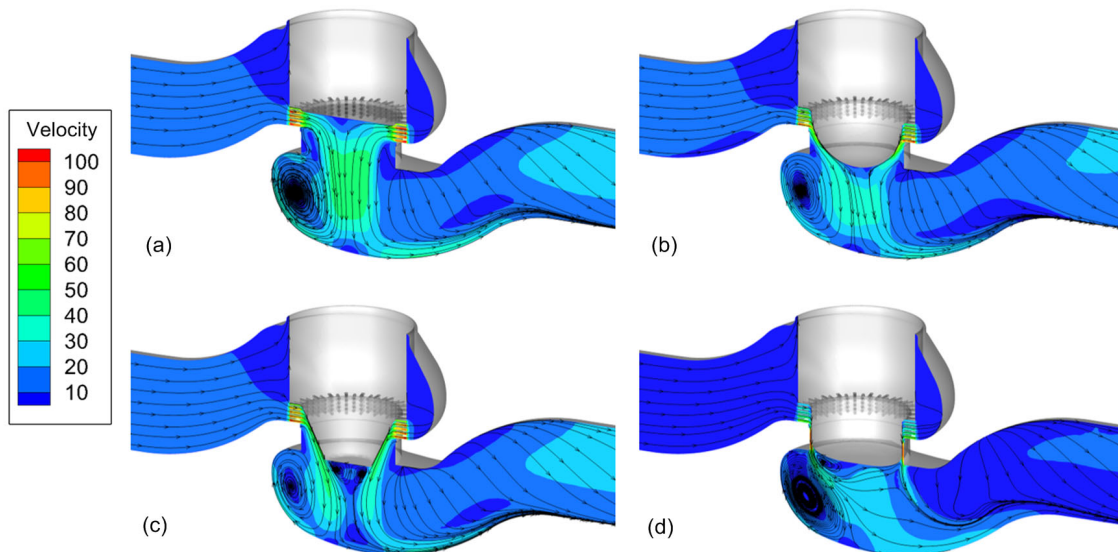


Fig. 5 Velocity (unit: m/s) contours inside the sleeve regulating valve with valve core displacement of 30 mm for different valve core shapes: (a) flat bottom; (b) ellipsoid; (c) circular truncated cone; (d) cylinder

higher than in the others, whether the valve core displacement is 60 mm or 30 mm. The throttling effects induced by the cylinder valve core are the strongest. The throttling effects of the valve with the flat bottom valve core are the weakest. The ranking is: flat bottom, circular truncated cone, ellipsoid, and cylinder. The same conclusion can also be seen in Fig. 6b. For the region at the center of the valve chamber, the velocity for the ellipsoid valve core is the highest when the

valve core displacement is 60 mm. However, when the valve core displacement is 30 mm, the velocity at the center of the valve chamber for the flat bottom valve core is the highest. Comparing Fig. 6a with Fig. 6b, it can be seen that the velocity for the valve core displacement of 30 mm is lower than that for the valve core displacement of 60 mm, not only at the inlet and outlet, but also at the center of the valve chamber. It can therefore be seen that the decrease of

valve core displacement induces an enhancement of the throttling effects of the valve.

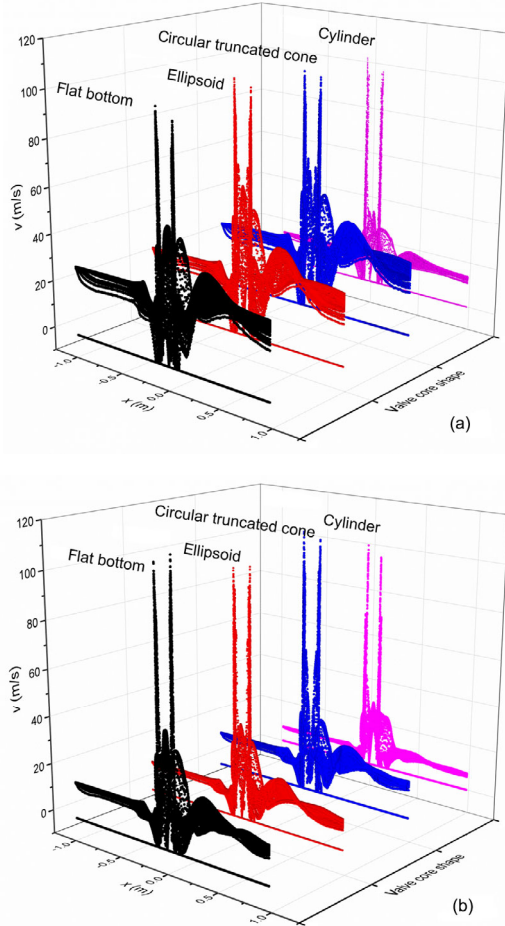


Fig. 6 Velocity (v) variation along the horizontal direction (x) for different valve core shapes
 (a) Valve core displacement of 60 mm; (b) Valve core displacement of 30 mm

Fig. 7 shows the mass flow rates (Q) of the sleeve regulating valve for different valve core shapes with the increase of the valve core displacement (L). It can be seen that the flux characteristic for the ellipsoid valve core is nearly linear. With the increase of the valve core displacement, the mass flow rate is increased linearly. The curves for the flat bottom and circular truncated cone valve cores are similar and convex when compared with the linear curve. With the increase of the valve core displacement, the increase velocity of the mass flow rate decreases gradually. For the cylinder valve core, the curve is close to an exponential one. With the increase in the valve core displacement, the increase velocity of the mass flow

rate increases gradually. It can be seen that the mass flow rate for the cylinder valve core is lower than those of all others at all valve core displacements, which shows that the throttling effect of the cylinder valve core is the strongest.

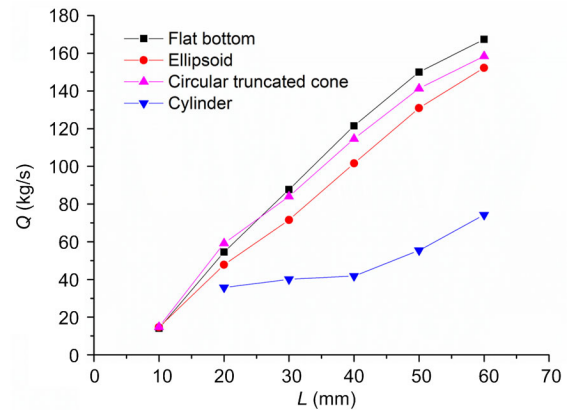


Fig. 7 Mass flow rates (Q) of the sleeve regulating valve with different valve core displacements (L) for different valve core shapes

3.2 Pressure difference analysis on cavitation flow

Fig. 8 depicts the pressure distributions in the symmetric cross section of valve for different valve core shapes when the valve core displacement is 60 mm, while Fig. 9 shows them for a valve core displacement of 30 mm.

For a valve core displacement of 60 mm, the pressures at the inlet of the regulating valve for all four valve core shapes remain stable above 8.00 MPa, while the pressures at the outlet of the sleeve regulating valve are kept below 2.50 MPa. When the fluid flows through the sleeve, the pressures experience totally different changes for the four different valve cores because of the different valve core shapes. For the flat bottom valve core, a sudden pressure decrease appears at the inlet of the orifices in the sleeve and the pressure decreases below 3.50 MPa. For the ellipsoid and circular truncated cone valve cores, the pressures experience a gradual change from the top to the bottom of the sleeve. For the cylinder valve core, the pressure drop only appears at the lower part of the sleeve, and the pressure at the upper part of the sleeve remains above 8.00 MPa. A sudden pressure drop appears in the throat between the wall of the valve core chamber and the valve core, and the pressure falls below 2.00 MPa. In the left side of the valve

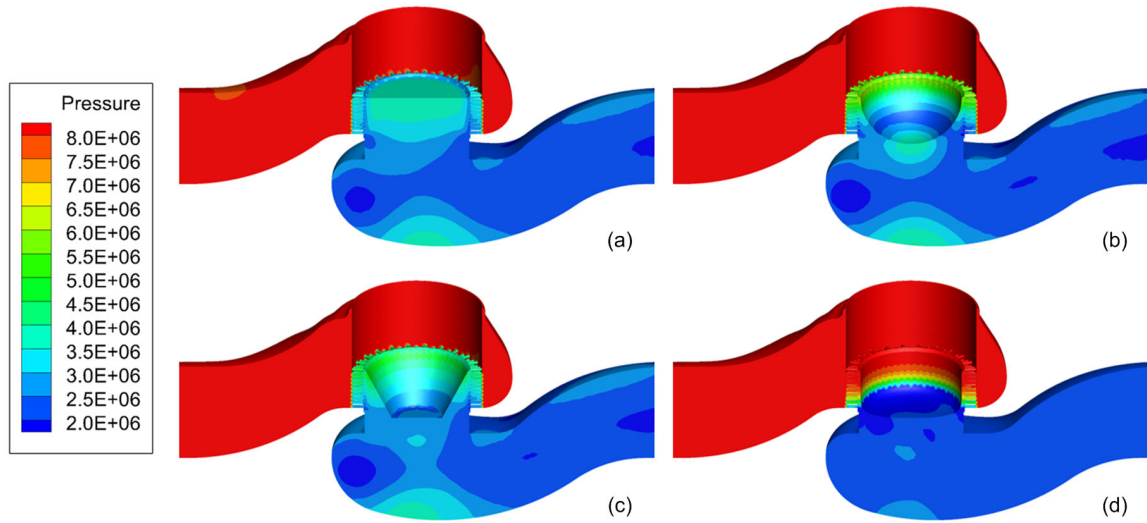


Fig. 8 Pressure (unit: Pa) contours inside the sleeve regulating valve with valve core displacement of 60 mm for different valve core shapes: (a) flat bottom; (b) ellipsoid; (c) circular truncated cone; (d) cylinder

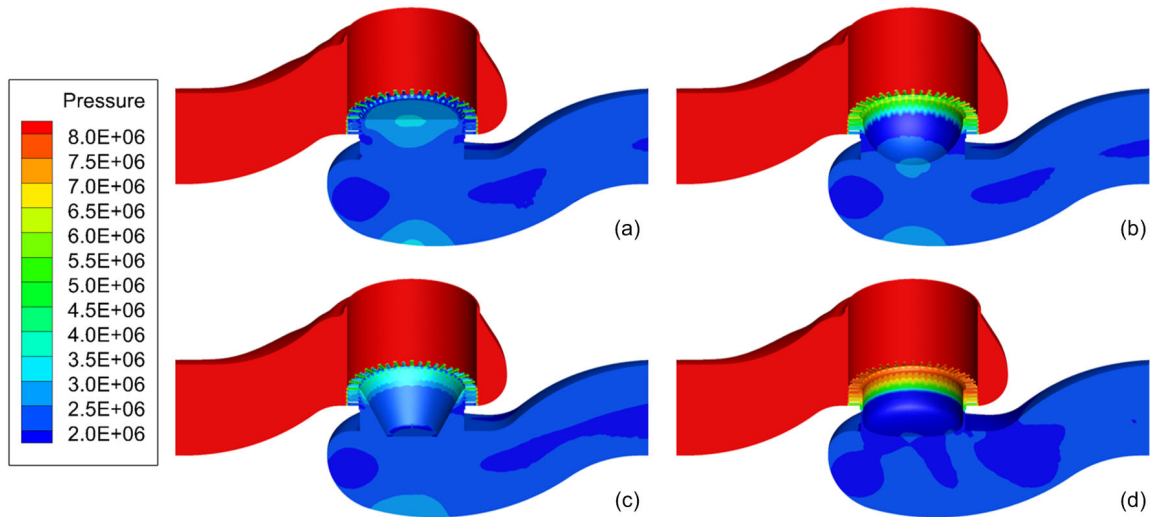


Fig. 9 Pressure (unit: Pa) contours inside the sleeve regulating valve with valve core displacement of 30 mm for different valve core shapes: (a) flat bottom; (b) ellipsoid; (c) circular truncated cone; (d) cylinder

chamber, there is always a region with low pressure below 2.00 MPa for the flat bottom, ellipsoid, and circular truncated cone valve cores. In comparison with Fig. 4, it can be found that there is always a vortex in the region with low pressure.

Considering the pressure distribution on the surface of the valve core, the pressure on the surface of the flat bottom valve core remains between 3.00 MPa and 4.00 MPa homogeneously. For the ellipsoid valve core, the pressure remains in a stepped circular distribution from the upper part to the bottom

of the valve core surface. For the valve with circular truncated cone valve core, a local region with low pressure appears at the edge between the conical surface and the bottom surface of the valve core, where cavitation easily occurs. As for the cylinder valve core, there is a large-area region with low pressure below 2.00 MPa on its bottom surface. In that region, cavitation may occur.

When the valve core displacement is decreased from 60 mm to 30 mm, the pressure distributions at the inlet and outlet of the valve still remain stable. For

the flat bottom and circular truncated cone valve cores, the pressure decreases when flowing through the sleeve are sudden and the pressures are lower than 3.50 MPa, while the decreases in pressure for the other two valve cores when the fluid flows through the sleeve are more gradual. Considering the local regions with pressure lower than 2.00 MPa where cavitation easily occurs, the region with lower pressure below 2.00 MPa for the flat bottom valve core is concentrated in the outlet of the orifice in the sleeve. For the circular truncated cone valve core, the region with pressure below 2.00 MPa is concentrated in the orifice outlet and the edge between the conical and bottom surfaces of the valve core. For the ellipsoid and cylinder valve cores, the regions with pressure below 2.00 MPa both appear in the gap between the sleeve outlet and the valve core surface. The lower-pressure region in the left side of the valve chamber is related to the vortex in that region.

Fig. 10 depicts the pressure variation along the horizontal direction for different valve core shapes when the valve core displacements are 60 mm and 30 mm. When the valve core displacement is 60 mm, the inlet pressure for the cylinder valve core is slightly higher than for the other valves and the pressure at the center of the valve chamber is lower than in the other valves. When the fluid flows through the sleeve, the pressure for the cylinder valve core is decreased below 1.50 MPa, which may induce serious cavitation. For the valve core displacement of 30 mm, the pressure variations along the horizontal direction for all four valve cores are nearly overlapped, except for the pressures at the center of the valve chamber. When the fluid flows through the sleeve, the pressures for all four valve cores decrease below 1.50 MPa, which are different from the pressures at the valve core displacement of 60 mm.

3.3 Cavitation analysis in the sleeve regulating valve

Fig. 11 shows the vapor distribution induced by cavitation for different valve core shapes when the valve core displacement is 60 mm. In general, when cavitation causes severe valve damage, the vapor volume fraction of each computational cell, α , is higher than 0.5. Figs. 11a–11d depict the 3D isurfaces of α larger than 0.5 in valves with the valve core displacement of 60 mm for different valve core shapes.

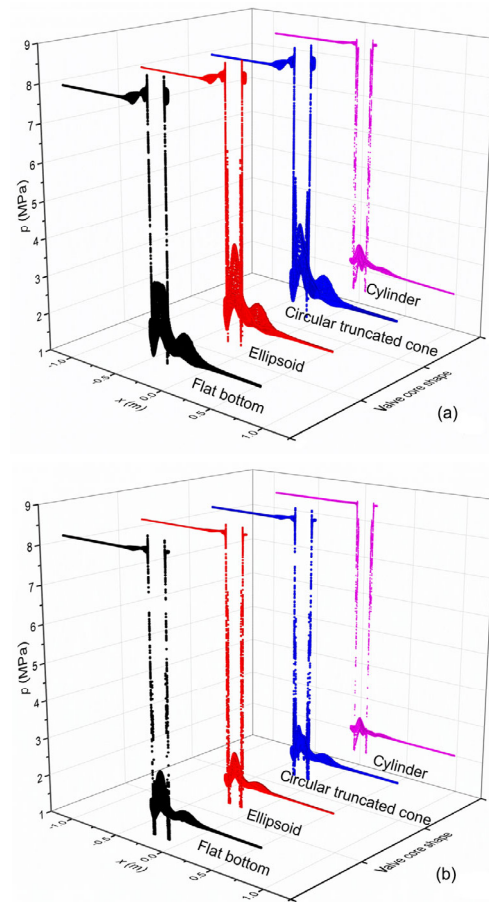


Fig. 10 Pressure (p) variation along the horizontal direction (x) for different valve core shapes

(a) Valve core displacement of 60 mm; (b) Valve core displacement of 30 mm

In general, for a regulating valve with a sleeve, the vapor caused by cavitation is mainly concentrated in the orifices of the sleeve because of its throttling effects. That is the phenomenon we hope to see as we can easily replace the sleeve during maintenance of the valve. However, in this study the introduction of valve cores with different shapes causes some differences especially at small openings.

Firstly, the valve with the valve core displacement of 60 mm is considered. For the flat bottom valve core, the vapor induced by cavitation inside the valve is mainly concentrated in the orifice inlet of the sleeve and the vapor distribution region is very small. When introducing the ellipsoid valve core, the vapor distribution region is changed. The vapor is concentrated in the orifice outlet located at the lower part of the sleeve and the vapor distribution is denser than that for the flat bottom valve core. There is no vapor

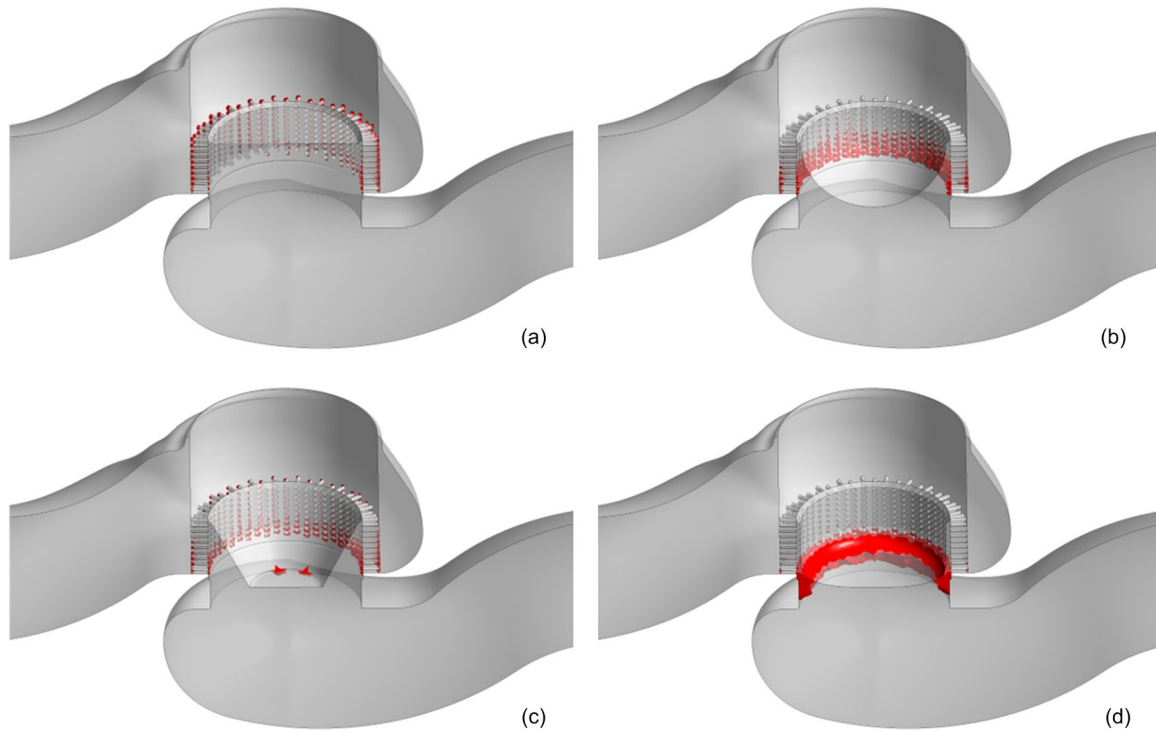


Fig. 11 Vapor distributions inside the sleeve regulating valve for different valve core shapes with the valve core displacement of 60 mm

(a) Flat bottom; (b) Ellipsoid; (c) Circular truncated cone; (d) Cylinder

at the upper part of the sleeve. For the valve with the circular truncated cone valve core, as shown in Fig. 11c, the vapor is concentrated in the orifice inlet and outlet of the valve but the distribution region is smaller than for the valve with the ellipsoid valve core. Meanwhile, at the edge between the conical and bottom surfaces of the valve core, some vapor appears but the distribution region is small. Finally, as shown in Fig. 11d in the case of the cylinder valve core, the throat between the sleeve and the valve core surface is nearly filled with vapor. The distribution region is obviously bigger than those inside the valves with the other three valve cores.

When the valve core displacement is decreased from 60 mm to 30 mm, as shown in Fig. 12, some changes appear because of the relative change of the throttling effects of the valve induced by the valve core displacement. For the flat bottom valve core, the vapor induced by cavitation inside the valve is mainly concentrated in the orifice inlet and outlet of the sleeve. Not only the vapor distribution region but also the distribution density is higher than in the same valve at

a valve core displacement of 60 mm. For the ellipsoid valve core, the vapor almost occupies the gap between the sleeve and valve core surface, which means that the decrease of the valve core displacement induces more serious cavitation with the ellipsoid valve core. The vapor distribution for the circular truncated cone valve at a valve core displacement of 30 mm is similar to that at the maximum valve core displacement of 60 mm. However, the distribution density is denser than the distribution density at the maximum valve core displacement. For the cylinder valve core, the location of the vapor distribution is the same as the vapor distribution at the maximum valve core displacement. The vapor occupies the gap between the sleeve and valve core surface and is extended downward to the bottom of the valve core.

As a whole, a decrease in the valve core displacement enhances the intensity and density of cavitation. Comparing all the valve core displacements, the cavitation intensities for the ellipsoid and cylinder valve cores are more intense than for the flat bottom and circular truncated cone valve cores.

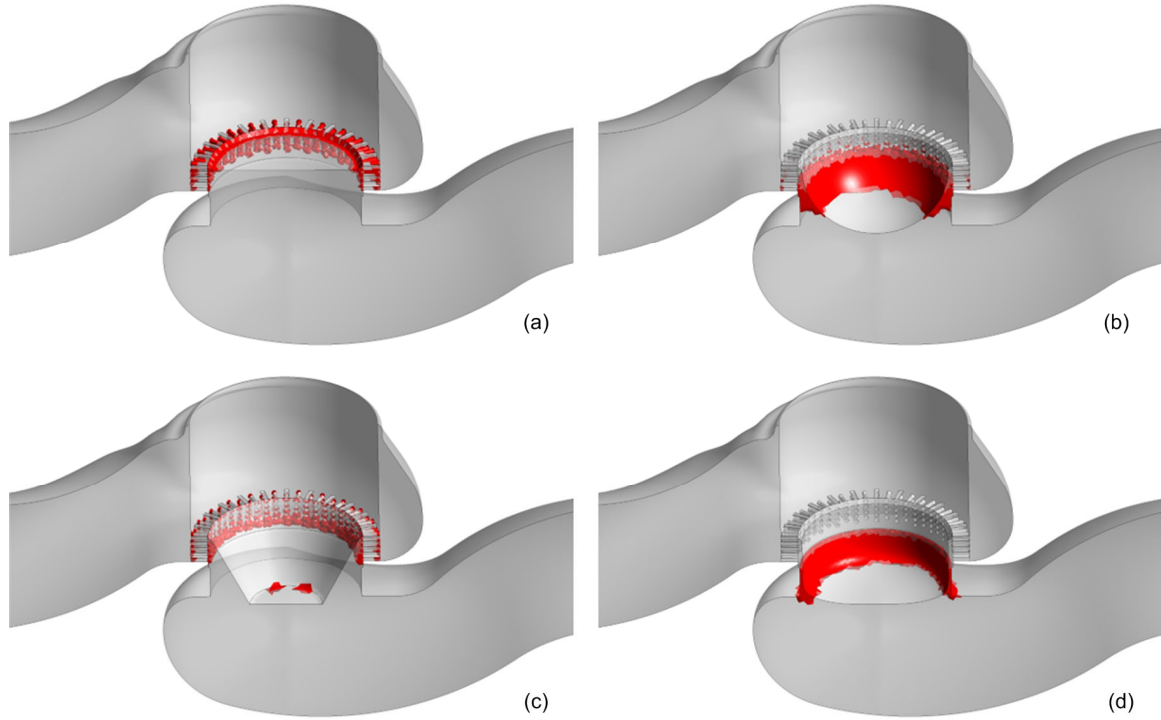


Fig. 12 Vapor distributions inside the sleeve regulating valve for different valve core shapes with the valve core displacement of 30 mm

(a) Flat bottom; (b) Ellipsoid; (c) Circular truncated cone; (d) Cylinder

To further quantify the influence of the valve core shapes on the cavitation characteristics of the sleeve regulating valve, the total vapor volume is also calculated by

$$V_v = \iiint_{\Omega} \alpha dV, \quad (5)$$

where α denotes the vapor volume fraction in an element, and Ω denotes the computational region. The total vapor volume represents the entire vapor caused by cavitation, so the total vapor volume represents the intensity of cavitation. The higher the total vapor volume is, the more intense the cavitation intensity is.

The total vapor volumes inside the valves for different valve core shapes at different valve core displacements are shown in Fig. 13. Considering the effect of the valve core shapes on total vapor volume, the total vapor volumes for the flat bottom and circular truncated cone valves are close and lower than 2500 mm^3 at all valve core displacements. It can be seen that the effects of the flat bottom and circular truncated cone valve cores on cavitation intensity are

identical. For the ellipsoid and cylinder valve cores, the total vapor volumes are much higher than those inside the valve for the other two valve cores at all valve core displacements. It is shown that the cavitation intensities for the ellipsoid and cylinder valve cores are more intense than those for the other two valve cores.

Then, the effects of valve core displacement on the total vapor volumes are analyzed. Overall, for all four valve core shapes, the total vapor volumes first increase and then decrease with the increase of the valve core displacement. However, for different valve core shapes, the corresponding valve core displacements of the maximum total vapor volume are different. For the flat bottom and ellipsoid valve cores, the corresponding valve core displacement of the maximum total vapor volume is 30 mm. It can be seen that the cavitation intensities for these two valve cores are the most intense when the valve core displacement is 30 mm. The maximum total vapor volume for the circular truncated cone valve core appears at a valve core displacement of 20 mm, while the maximum value for the cylinder valve core is at the valve core

displacement of 50 mm. Thus, the corresponding valve opening at maximum cavitation intensity is different for the different valve cores.

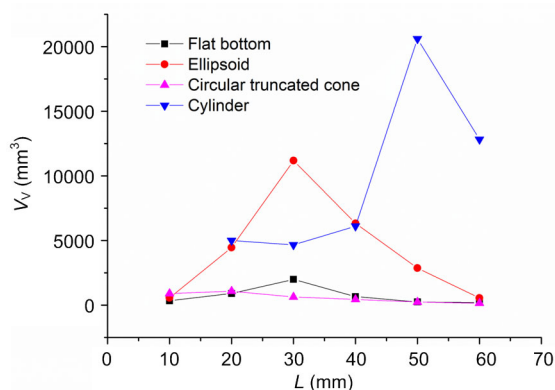


Fig. 13 Total vapor volumes (V_v) inside the valve for different valve core shapes and valve core displacements (L)

4 Conclusions

In this study, the cavitation occurring in a sleeve regulating valve with different valve core shapes for different valve core displacements has been numerically investigated, and the effects of valve core shapes that are flat bottom, ellipsoid, circular truncated cone, and cylinder have been revealed using the proposed numerical model.

First, the velocity distribution and the flow rates of the four different valve cores for different valve core displacements are analyzed. A high-velocity region appears behind the valve throat (sleeve) because the cross section shrinks for all four valve cores. According to the velocity difference between inlet and outlet, it is found that the throttling effect for the cylinder valve core is stronger than for the other three valve cores. With the decrease of the valve core displacement, the throttling effects for all four valve cores are enhanced. The flux characteristic for the ellipsoid valve core is close to linear while the flux characteristic for the cylinder valve core is close to exponential.

Then, the pressure differences inside the valves with different valve cores for different valve core displacements are analyzed. For the valve core displacement of 60 mm, a pressure drop to lower than 1.50 MPa only appears in the valve with the cylinder

valve core. With a decrease of the valve core displacement, a pressure drop to lower than 1.50 MPa appears in the valves with all four valve core shapes.

Lastly, the cavitation distribution and intensity are analyzed. For the flat bottom valve core, the vapor appears at the edge of the orifices in the sleeve. For the circular truncated cone valve core, the vapor appears at the edge of the orifices in the sleeve and at the bottom border of the valve core. For the ellipsoid and cylinder valve cores, the vapor distribution regions are concentrated in the gap between the sleeve and valve core. In total, the cavitation intensities for the ellipsoid and cylinder valve cores are more intense than the cavitation intensities for the other two valve cores. With the increase of the valve core displacement, the total vapor volumes for all four valve core shapes first increase and then decrease. As a whole, the flat bottom and circular truncated cone valve cores are recommended for their better performance in reducing cavitation.

Contributors

Chang QIU designed the research. Zhi-jiang JIN and Cheng-hang JIANG processed the corresponding data. Zhi-jiang JIN wrote the first draft of the manuscript. Jia-yi WU and Jin-yuan QIAN helped to organize the manuscript. Zhi-jiang JIN and Chang QIU revised and edited the final version.

Conflict of interest

Zhi-jiang JIN, Chang QIU, Cheng-hang JIANG, Jia-yi WU, and Jin-yuan QIAN declare that they have no conflict of interest.

References

- Baran G, Catana I, Magheti I, et al., 2010. Controlling the cavitation phenomenon of evolution on a butterfly valve. *IOP Conference Series: Earth and Environmental Science*, 12(1):012100. <https://doi.org/10.1088/1755-1315/12/1/012100>
- Chern MJ, Hsu PH, Cheng YJ, et al., 2013. Numerical study on cavitation occurrence in globe valve. *Journal of Energy Engineering*, 139(1):25-34. [https://doi.org/10.1061/\(ASCE\)EY.1943-7897.0000084](https://doi.org/10.1061/(ASCE)EY.1943-7897.0000084)
- Corbera S, Olazagoitia JL, Lozano JA, 2016. Multi-objective global optimization of a butterfly valve using genetic algorithms. *ISA Transactions*, 63:401-412. <https://doi.org/10.1016/j.isatra.2016.03.008>
- Deng J, Pan DY, Xie FF, et al., 2015. Numerical investigation of cavitation flow inside spool valve with large pressure drop. *Journal of Physics: Conference Series*, 656(1): 012067.

- https://doi.org/10.1088/1742-6596/656/1/012067
- Edvardsen S, Dorao CA, Nydal OJ, 2015. Experimental and numerical study of single-phase pressure drop in down-hole shut-in valve. *Journal of Natural Gas Science and Engineering*, 22:214-226.
https://doi.org/10.1016/j.jngse.2014.11.034
- Fu YK, Liu QY, Wang GR, et al., 2013. Mathematical modeling and validation on a new valve core of the throttle valve in MPD. *Advances in Mechanical Engineering*, 2013:125936.
https://doi.org/10.1155/2013/125936
- Gao H, Lin W, Tsukiji T, 2006. Investigation of cavitation near the orifice of hydraulic valves. *Proceedings of the Institution of Mechanical Engineers, Part G: Journal of Aerospace Engineering*, 220(4):253-265.
https://doi.org/10.1243/09544100JAERO26
- Hassis H, 1999. Noise caused by cavitating butterfly and monovar valves. *Journal of Sound and Vibration*, 225(3): 515-526.
https://doi.org/10.1006/jsvi.1999.2254
- Herbertson LH, Reddy V, Manning KB, et al., 2006. Wavelet transforms in the analysis of mechanical heart valve cavitation. *Journal of Biomechanical Engineering*, 128(2): 217-222.
https://doi.org/10.1115/1.2165694
- Hou CW, Qian JY, Chen FQ, et al., 2018. Parametric analysis on throttling components of multi-stage high pressure reducing valve. *Applied Thermal Engineering*, 128:1238-1248.
https://doi.org/10.1016/j.applthermaleng.2017.09.081
- Huovinen M, Kolehmainen J, Koponen P, et al., 2015. Experimental and numerical study of a choke valve in a turbulent flow. *Flow Measurement and Instrumentation*, 45:151-161.
https://doi.org/10.1016/j.flowmeasinst.2015.06.005
- Jia WH, Yin CB, 2010. Numerical analysis and experiment research of cylinder valve port cavitating flow. *Proceedings of SPIE 7522, Fourth International Conference on Experimental Mechanics*, Article 75225X.
https://doi.org/10.1117/12.849216
- Jin ZJ, Gao ZX, Qian JY, et al., 2018. A parametric study of hydrodynamic cavitation inside globe valve. *Journal of Fluids Engineering*, 140(3):031208.
https://doi.org/10.1115/1.4038090
- Kudźma Z, Stosiak M, 2015. Studies of flow and cavitation in hydraulic lift valve. *Archives of Civil and Mechanical Engineering*, 15(4):951-961.
https://doi.org/10.1016/j.acme.2015.05.003
- Li SJ, Aung NZ, Zhang SZ, et al., 2013. Experimental and numerical investigation of cavitation phenomenon in flapper-nozzle pilot stage of an electrohydraulic servo-valve. *Computers & Fluids*, 88:590-598.
https://doi.org/10.1016/j.compfluid.2013.10.016
- Lisowski E, Filo G, 2016. CFD analysis of the characteristics of a proportional flow control valve with an innovative opening shape. *Energy Conversion and Management*, 123: 15-28.
https://doi.org/10.1016/j.enconman.2016.06.025
- Liu Q, Ye JH, Zhang G, et al., 2019. Study on the metrological performance of a swirlmeter affected by flow regulation with a sleeve valve. *Flow Measurement and Instrumentation*, 67:83-94.
https://doi.org/10.1016/j.flowmeasinst.2019.04.003
- Liu YH, Ji XW, 2009. Simulation of cavitation in rotary valve of hydraulic power steering gear. *Science in China Series E: Technological Sciences*, 52(11):3142-3148.
https://doi.org/10.1007/s11431-009-0277-z
- Lu L, Xie SH, Yin YB, et al., 2020. Experimental and numerical analysis on the surge instability characteristics of the vortex flow produced large vapor cavity in u-shape notch spool valve. *International Journal of Heat and Mass Transfer*, 146:118882.
https://doi.org/10.1016/j.ijheatmasstransfer.2019.118882
- Nie SL, Huan GH, Li YP, et al., 2006. Research on low cavitation in water hydraulic two-stage throttle poppet valve. *Proceedings of the Institution of Mechanical Engineers, Part E: Journal of Process Mechanical Engineering*, 220(3):167-179.
https://doi.org/10.1243/09544089JPME78
- Okita K, Miyamoto Y, Kataoka T, et al., 2015. Mechanism of noise generation by cavitation in hydraulic relief valve. *Journal of Physics: Conference Series*, 656(1):012104.
https://doi.org/10.1088/1742-6596/656/1/012104
- Ou GF, Xu J, Li WZ, et al., 2015. Investigation on cavitation flow in pressure relief valve with high pressure differentials for coal liquefaction. *Procedia Engineering*, 130: 125-134.
https://doi.org/10.1016/j.proeng.2015.12.182
- Qian JY, Wei L, Jin ZJ, et al., 2014. CFD analysis on the dynamic flow characteristics of the pilot-control globe valve. *Energy Conversion and Management*, 87:220-226.
https://doi.org/10.1016/j.enconman.2014.07.018
- Qian JY, Hou CW, Wu JY, et al., 2019a. Aerodynamics analysis of superheated steam flow through multi-stage perforated plates. *International Journal of Heat and Mass Transfer*, 141:48-57.
https://doi.org/10.1016/j.ijheatmasstransfer.2019.06.061
- Qian JY, Gao ZX, Hou CW, et al., 2019b. A comprehensive review of cavitation in valves: mechanical heart valves and control valves. *Bio-Design and Manufacturing*, 2(2): 119-136.
https://doi.org/10.1007/s42242-019-00040-z
- Qian JY, Wu JY, Gao ZX, et al., 2019c. Hydrogen decomposition analysis by multi-stage Tesla valves for hydrogen fuel cell. *International Journal of Hydrogen Energy*, 44(26):13666-13674.
https://doi.org/10.1016/j.ijhydene.2019.03.235
- Qian JY, Chen MR, Gao ZX, et al., 2019d. Mach number and energy loss analysis inside multi-stage Tesla valves for hydrogen decompression. *Energy*, 179:647-654.

- <https://doi.org/10.1016/j.energy.2019.05.064>
 Qian JY, Chen MR, Liu XL, et al., 2019e. A numerical investigation of the flow of nanofluids through a micro Tesla valve. *Journal of Zhejiang University-SCIENCE A (Applied Physics & Engineering)*, 20(1):50-60.
<https://doi.org/10.1631/jzus.A1800431>
- Qu WS, Tan L, Cao SL, et al., 2015. Experiment and numerical simulation of cavitation performance on a pressure-regulating valve with different openings. *IOP Conference Series: Materials Science and Engineering*, 72(4): 042035.
<https://doi.org/10.1088/1757-899X/72/4/042035>
- Schnerr GH, Sauer J, 2001. Physical and numerical modeling of unsteady cavitation dynamics. Proceedings of the 4th International Conference on Multiphase Flow.
- Shi WJ, Cao SP, Luo XH, et al., 2017. Experimental research on the cavitation suppression in the water hydraulic throttle valve. *Journal of Pressure Vessel Technology*, 139(5):051302.
<https://doi.org/10.1115/1.4037443>
- Tao JY, Lin Z, Ma CJ, et al., 2020. An experimental and numerical study of regulating performance and flow loss in a V-port ball valve. *Journal of Fluids Engineering*, 142(2): 021207.
<https://doi.org/10.1115/1.4044986>
- Ulanicki B, Picinali L, Janus T, 2015. Measurements and analysis of cavitation in a pressure reducing valve during operation—a case study. *Procedia Engineering*, 119:270-279.
<https://doi.org/10.1016/j.proeng.2015.08.886>
- Wang C, Hu B, Zhu Y, et al., 2019. Numerical study on the gas-water two-phase flow in the self-priming process of self-priming centrifugal pump. *Processes*, 7(6):330.
<https://doi.org/10.3390/pr7060330>
- Wang GR, Tao SY, Liu QY, et al., 2014. Experimental validation on a new valve core of the throttle valve in managed pressure drilling. *Advances in Mechanical Engineering*, 2014:324219.
<https://doi.org/10.1155/2014/324219>
- Xu YQ, Guan ZC, Liu YW, et al., 2014. Structural optimization of downhole float valve via computational fluid dynamics. *Engineering Failure Analysis*, 44:85-94.
<https://doi.org/10.1016/j.engfailanal.2014.04.033>
- Yaghoubi H, Madani SAH, Alizadeh M, 2018. Numerical study on cavitation in a globe control valve with different numbers of anti-cavitation trims. *Journal of Central South University*, 25(11):2677-2687.

- <https://doi.org/10.1007/s11771-018-3945-y>
 Zhang ZT, Cao SP, Luo XH, et al., 2017. New approach of suppressing cavitation in water hydraulic components. *Proceedings of the Institution of Mechanical Engineers, Part C: Journal of Mechanical Engineering Science*, 231(21):4022-4034.
<https://doi.org/10.1177/0954406216657847>

中文概要

题目: 阀芯形状对套筒式调节阀内空化流动的影响研究

目的: 套筒式调节阀内空化的发生不仅会增加整个管路系统的能量损耗,而且会造成阀体及管路的失效破坏。本文旨在探讨四种不同形状的阀芯对套筒式调节阀内不同阀芯位移工况下的空化流动及空化强度的影响,为套筒式调节阀的优化设计及空化控制提出建议。

创新点: 1. 根据四种不同形状的阀芯,研究套筒式调节阀内阀芯形状对流动及空化特性的影响; 2. 建立数值模型,对套筒式调节阀在不同阀芯形状和不同阀芯位移条件下进行流动及空化分析。

方法: 1. 建立带有不同形状阀芯的套筒式调节阀数值计算模型,并比较分析阀芯形状对阀内速度、压力及空化情况的影响(图4, 8和11); 2. 建立不同阀芯位移条件下的阀门数值模型,比较分析阀芯位移对阀内速度、压力及空化情况的影响(图6和10); 3. 建立不同形状阀芯及不同阀芯位移下的阀门模型,分析阀芯形状和位移对阀内流动及空化特性的综合影响(图7和13)。

结论: 1. 在四种不同形状阀芯的条件下,高速流动区域和空化发生区主要位于套筒与阀芯之间的间隙; 2. 在直筒形和椭球形阀芯条件下的阀内空化强度明显强于平底形和圆台形阀芯条件下的空化强度,因此平底形和圆台形阀芯在空化控制方面具有更好的效果; 3. 在四种不同形状阀芯的条件下,随着阀芯位移的增加,阀内由空化产生的蒸汽总体积先增加后减少。

关键词: 套筒式调节阀; 空化强度; 阀芯形状; 总体蒸汽体积